Bioorganic & Medicinal Chemistry Letters 21 (2011) 5633–5637

Contents lists available at ScienceDirect

Bioorganic & Medicinal Chemistry Letters

journal homepage: www.elsevier.com/locate/bmcl

Design, synthesis, and biological evaluation of pyrazolopyrimidine-sulfonamides as potent multiple-mitotic kinase (MMK) inhibitors (part I)

Lin Zhang [a,*], Junhua Fan [a], Jer-Hong Chong [a], Angela Cesena [a], Betty Y. Y. Tam [a], Charles Gilson [a], Christina Boykin [a], Deping Wang [b], Dikran Aivazian [a], Doug Marcotte [b], Guangqing Xiao [b], Jean-Yves Le Brazidec [a], Jinhua Piao [a], Karen Lundgren [a], Kevin Hong [a], Khang Vu [a], Khanh Nguyen [a], Liang-Shang Gan [b], Laura Silvian [b], Leona Ling [b], Min Teng [a], Mitchell Reff [a], Nicole Takeda [a], Noel Timple [a], Qin Wang [b], Ron Morena [a], Samina Khan [a], Shuo Zhao [a], Tony Li [a], Wen-Cherng Lee [b], Arthur G. Taveras [b], Jianhua Chao [a]

[a] Biogen Idec, 5200 Research Place, San Diego, CA 92122, United States
[b] Biogen Idec, 12 Cambridge Center, Cambridge, MA 02142, United States

ARTICLE INFO

Article history:
Received 4 April 2011
Revised 7 June 2011
Accepted 10 June 2011
Available online 13 July 2011

Keyword:
Kinase inhibitors

ABSTRACT

A novel class of pyrazolopyrimidine-sulfonamides was discovered as selective dual inhibitors of aurora kinase A (AKA) and cyclin-dependent kinase 1 (CDK1). These inhibitors were originally designed based on an early lead (compound **I**). SAR development has led to the discovery of potent inhibitors with single digit nM IC_{50}s towards both AKA and CDK1. An exemplary compound **1a** has demonstrated good efficacy in an HCT116 colon cancer xenograft model.

Mitotic kinases play important roles in the development and progression of cancer by acting as key regulators of cell proliferation. There are three families of serine/threonine mitotic kinases: aurora kinases (AKA, AKB, and AKC),[1] polo-like kinases (PLK1),[2] and cyclin-dependent kinases (CDK1).[3] These mitotic kinases are involved in cell cycle arrest and apoptosis of tumor cells, and frequently overexpressed in many tumors. Inhibition of any single mitotic kinase could lead to inhibition of tumor growth; inhibiting multiple mitotic kinases (MMK) simultaneously may present a particularly unique opportunity in cancer therapy. These MMK inhibitors can be used as a single agent or in combination with other G2/M active agents. In our search of small molecule inhibitors targeting AKA/AKB and CDK1, we have identified a novel class of pyrazolopyrimidine-sulfonamides as potent inhibitors. Herein we report our results and findings.

A number of aurora kinase inhibitors have been reported in literatures, which have demonstrated anti-tumor activities in preclinical models. A few of them have entered clinical evaluations, including VX-680, AZD1152, and MLN8237 (Fig. 1).[4–6] CDK inhibitors such as R547 have also demonstrated anti-tumor activities and have been evaluated in clinical trials.[7] In our earlier disclosure,[8]

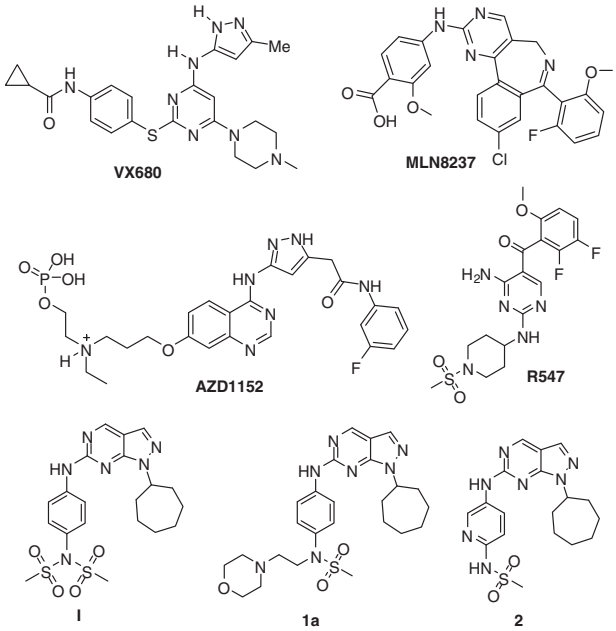

Figure 1. Structures of **VX680**, **MLN8237**, **AZD1152**, **R547**, **I**, **1a** and **2**.

* Corresponding author.
E-mail address: lin.zhang.ge@sbcglobal.net (L. Zhang).

0960-894X/$ - see front matter © 2011 Elsevier Ltd. All rights reserved.
doi:10.1016/j.bmcl.2011.06.129

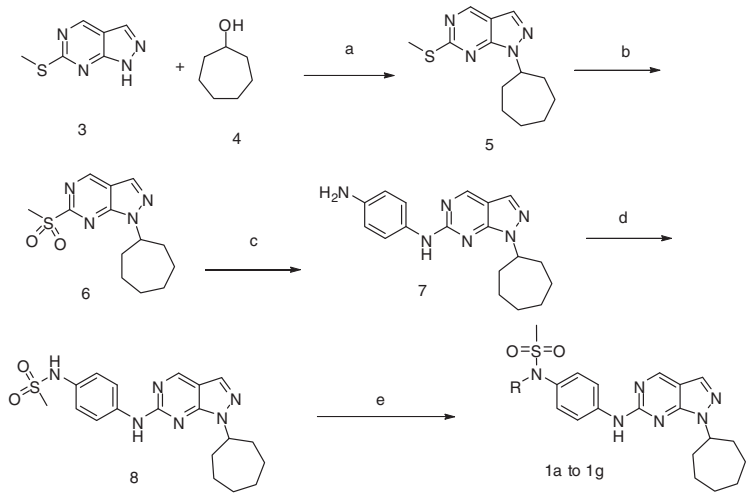

Scheme 1. Synthesis of pyrazolo-pyrimidines **1**. Reagents and conditions: (a) DIAD, PPh_3, THF, −70 °C to rt, 65%; (b) oxone, 1:1 MeOH/H_2O, rt, 85%; (c) benzene-1,4-diamine, DMSO, 120 °C, 78%; (d) CH_3SO_2Cl, DIEA, $CHCl_3$, rt, 87%; (e) RCl, K_2CO_3, DMF, 70 °C, 30–85%.

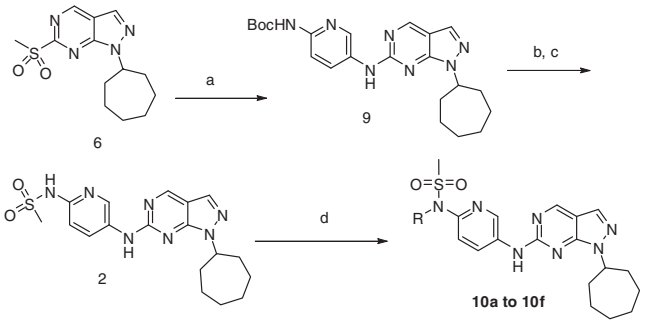

Scheme 2. Synthesis of **10**. Reagents and conditions: (a) 2-Bocamino-5-amino pyridine, DMSO, 120 °C, 70%; (b) TFA, CH_2Cl_2, rt, 95%; (c) CH_3SO_2Cl, DIEA, $CHCl_3$, rt, 86%; (d) RCl, K_2CO_3, DMF, 70 °C, 30–87%.

we mentioned bissulfonamide compounds such as **I** (Fig. 1) which were capable of inhibiting both aurora and CDK1 kinases and acting as an MMK inhibitor.

Compounds from the bissulfonamide class have generally exhibited poor solubility. To improve physiochemical properties and inhibitory activities, we modified the bissulfonamide scaffold of I and discovered that mono-sulfonamide-phenyl pyrazolopyrimidine analogs such as **1a** improve solubility while maintaining inhibition of both aurora and CDK kinases in biochemical and cellular assays. Furthermore, our SAR studies led us to mono-pyridyl sulfonamides as represented by **2** and **10**, which have demonstrated improved drug properties with comparable inhibitory activities to the mono-sulfonamide-phenyl class.

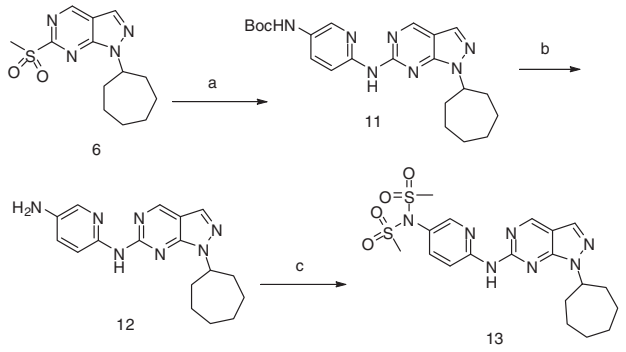

Scheme 3. Reagents and conditions: (a) *tert*-butyl 6-aminopyridin-3-ylcarbamate, DMSO, 120 °C, 65%; (b) TFA, CH_2Cl_2, rt, 90%; (c) CH_3SO_2Cl (2 equiv), DIEA, $CHCl_3$, rt, 72%.

The synthesis of monosulfonamidophenyl pyrazolo-pyrimidine series of compounds **1** (**a**–**g**) was outlined in Scheme 1. Starting with thiomethyl pyrazolopyrimidine **3** and cycloheptanol **4**, key building block **5** was prepared using the procedures described by Adams.[9] Oxidation of **5** using Oxone® afforded methyl sulfone **6**, which was subsequently converted to phenylaniline intermediate **7** by reacting with 1,4-diaminobenzene under a standard condition (DMSO, 120 °C). Treatment of **7** with methanesulfonyl chloride under a mild basic condition (DIEA) resulted in monomethylsulfonamide **8**. Compound **8** has served as a template for SAR exploration. A variety of N-substituted mono-sulfonamides **1** were prepared by reacting **8** with appropriate halides in the presence of K_2CO_3 at an elevated temperature.

The synthetic approach used for the preparation of mono-sulfonamide-pyridyl pyrazolo-pyrimidine analogs **10** is summarized in Scheme 2. Methylsulfone intermediate **6** was reacted with 2-Boc-amino-5-amino pyridine under elevated temperature to afford key pyridyl intermediate **9**. By removing the Boc protection group followed by sulfonylation, **9** was converted to mono-methylsulfonamide **2**. N-Alkylation of **2** with various halides afforded the desired pyridyl analogs **10** (**a**–**f**).

To investigate the biochemical and cellular activities of this compound class, the pyridyl nitrogen was positioned at different locations within the ring. The 2-pyridyl bissulfonamide **13** can be compared directly to both the earlier phenyl lead **I** (Fig. 1) and to the 3-pyridyl analogs **10 (a–f)**. The 2-pyridyl 5-bissulfonamide compound **13** was prepared following the route depicted in Scheme 3. Displacement of the sulphone moiety in methyl sulphone **6** with 2-amino-5-boc-amino pyridine yielded **11**. Upon deprotection and reaction with methanesulfonyl chloride, 3-pyridyl bissulfonamide **13** was obtained.

The biochemical and cellular activities of the N-substituted mono-sulfonamido-phenyl analogs **1** are summarized in Table 1. Compounds **1a**, **1b**, **1c**, **1e**, **1f**, and **1h** demonstrate potent enzymatic inhibition, with single digit or low double digit nM potency against AKA and CDK1 in biochemical FRET assays.[10] In a G2/M cell cycle arrest assay, where flow cytometry is used to measure the degree of G2/M arrest in K562 cells,[11] these compounds exhibited inhibitory IC_{50}s below 100 nM. Compounds **1d** and **1g** showed slightly weaker activity in the G2/M arrest assay (IC_{50} of 300 nM) or in the MTS phenotypic growth assay compared to the others

Table 1
AKA, CDK1, G2M arrest and MTS assay results for compounds **1a**–**1h**

No.	R	AKA[a] IC_{50} (μM)	CDK[b] IC_{50} (μM)	G2M[c] IC_{50} (μM)	MTS[d] IC_{50} (μM)
1a	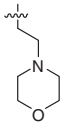	0.014	0.023	0.10	0.160
1b	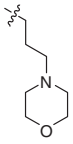	0.005	0.005	0.10	0.170
1c		0.006	0.006	0.10	0.078
1d		0.005	0.09	0.30	0.240
1e		0.013	0.005	0.03	0.077
1f		0.020	0.005	0.10	0.060
1g	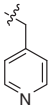	0.030	0.023	0.30	0.250
1h	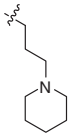	0.009	0.006	0.10	0.092

[a] AKA inhibition assay, measures inhibition of phosphorylation of a Lats2 substrate protein by aurora kinase A protein.
[b] CDK1 inhibition assay, a FRET-based assay that measures inhibition of phosphorylation of a peptide substrate by CDK1/cyclin B.
[c] G2/M cell cycle arrest assay, a flow cytometric assay for measuring the percentage of cells in G2/M arrest after treatment with mitotic kinase inhibitors.
[d] MTS assay for cellular cytotoxicity in HCT116 cells, a phenotypic cellular assay, which measures growth inhibition in cells treated with inhibitors.[12]

Table 2
AKA, CDK1, G2M arrest and MTS assay results for compounds **10a** to **10f**, and **13**

No.	R	AKA[a] IC_{50} (μM)	CDK [b] IC_{50} (μM)	G2M[c] IC_{50} (μM)	MTS[d] IC_{50} (μM)
2	H	0.017	0.007	0.3	0.210
10a	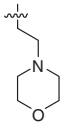	0.150	0.031	2.0	0.500
10b		0.350	0.010	1.0	0.125
10c		0.260	0.010	0.3	0.220
10d		0.110	0.004	0.3	0.145
10e		0.180	0.003	0.3	0.119
10f	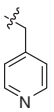	0.095	0.013	0.3	0.320
13		>10	>10	>3	N/A

[a–d] See footnote under Table 1.

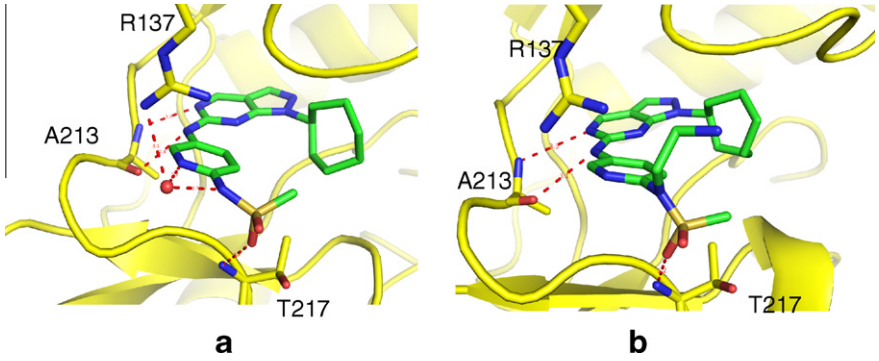

Figure 2. X-ray structure of inhibitors **2** and **10e** in aurora A (2.8 Å). Graphics were prepared using PyMOL.[14]

Table 3
ADMET properties of compound **1a** and **2**

No.	Caco-2 Papp ($\times 10^{-6}$ cm/s) AP to BL	Efflux ratio	LM stability $\%Q_h$ M/R/H	CYP IC_{50} (μM)	hERG% inh (10 μM)
1a	26.5	1.1	96/94/95	3A4 = 0.04 2C19 = 0.03 2C9 = 0.001 2D6 and 1A2 >10	40
2	20.1	1.5	33/30/39	3A4, 2D6, 1A2, 2C9, 2C19 >10	6.5

in this series. In general, analogs with smaller N-substituents (R) are more potent in both biochemical assays against AKA and CDK1 and in cellular assays.

The in vitro activity data of N-substituted mono-sulfonamido-pyridyl analogs **10** was reported in Table 2. 2-Pyridyl sulfonamides generally maintained biochemical activities, though weaker than the corresponding phenyl analogs (**1**). However, the placement of nitrogen was important. Moving the nitrogen from the *ortho* position of the sulfonamide (**10**) to the *meta* position (**13**) resulted in a loss of all activity. This is likely due to the unfavorable electrostatic repulsion between the hinge and the nitrogen at this position.

In the pyridyl series, the requirement of the N-substituent group was slightly different from the phenyl series, and the unsubstituted (R = H) mode seemed to be preferred. This was particularly evident in monitoring the AKA inhibitory activity, as compound **2** exhibited the most potent AKA inhibition observed to date. Co-crystal structures of compounds **2** and **10e** with AKA were obtained (Fig. 2, **a** and **b**) to provide insight into the SAR observed.[13] The N of pyridine in compound **2** can form water-bridged hydrogen bonds with both R137 and the NH of the sulfonamide. In contrast, no sulfonamide proton is available for the water-bridged hydrogen bond network in compound **10e**, and the water is also not observed in electron density maps. This difference in water structure could explain the 10-fold more potent activity observed for compound **2**.

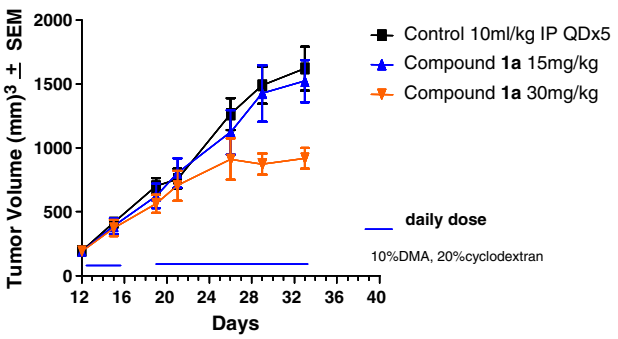

Figure 3. Efficacy results of **1a** in HCT116 nu/nu mouse tumor xenograft models.

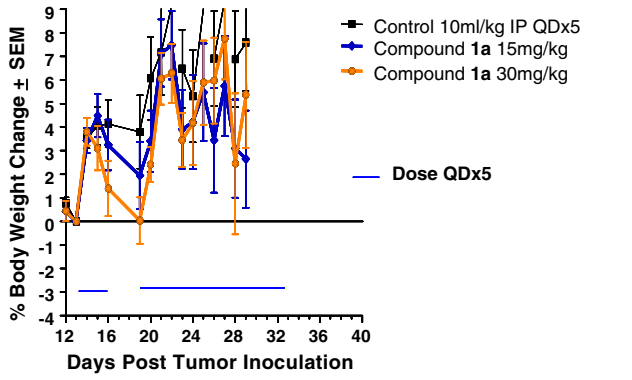

Figure 4. Body weight change after administration of **1a** in HCT116 nu/nu mouse models.

We speculated that the diaminophenyl arrangement in compounds like **1** may lead to the generation of reactive metabolites while in the pyridyl analogs, this problem could be alleviated. The pyridyl compound **2** also exhibited improved pharmacokinetic properties (Table 3). Both phenyl compound **1a** and pyridyl analog **2** were compared in Caco-2 cell permeability assays,[15] liver microsome stability assays,[16] CYP[17] and hERG[18] inhibition assays. Compound **1a** showed high clearance in mouse, rat and human liver microsomes. In contrast, compound **2** was quite stable, with a $\%Q_h$ in the range of 30–40% hepatic blood flow for mouse, rat and human liver microsomes. The phenyl compound **1a** has metabolic liabilities, as it inhibits CYP450s (3A4, 2C19 and 2C9) and hERG channels at <10 μM concentrations. The pyridyl compound **2**, on the other hand, was less encumbered by these issues.

To establish a correlation between in vitro and in vivo activity, an early lead compound phenyl sulfonamide **1a** was evaluated in an HCT116 mouse colon xenograft mouse model. This compound demonstrated a 50% tumor growth inhibition without causing body weight loss after a 21-day treatment regime (IP, daily, Figs. 3 and 4). This result was encouraging as we continue our efforts in modifying the compounds to achieve better in vitro activity and an improved metabolic profile, ultimately to realize better in vivo efficacy.

In conclusion, a novel class of pyrazolopyrimidine-sulfonamides (phenyl **1** or pyridyl **10**) was identified, which shows dual inhibition of aurora kinase A (AKA) and cyclin-dependent kinase 1 (CDK1). The analogs generally have good enzymatic and cellular inhibitory activities. The N-substituted mono-sulfonamidophenyl analogs are more potent in cellular phenotypic and G2/M arrest assays than the N-substituted mono-sulfonamidopyridyl analogs but the pyridyl analogs have better metabolic properties. The pyridyl nitrogen *ortho* to the sulfonyl group is required to maintain activity. A prototypic compound (**1a)** demonstrated encouraging efficacy in an HCT116 colon cancer xenograft model, which warrants further SAR development of this class of MMK inhibitors.

Acknowledgments

Special thanks to Dr. Adeela Kamal, Dr. Srinivas R. Kasibhatla, Dr. Francis J. Burrows, and Dr. Marcus F. Boehm for their contributions to this program.

References and notes

1. Andrews, P. D.; Knatko, E.; Moore, W. J.; Swedlow, J. R. *Curr. Opin. Cell Biol.* **2003**, *15*, 672.
2. Steegmaier, M.; Hoffmann, M.; Baum, A.; Lénárt, P.; Petronczki, M.; Krssák, M.; Gürtler, U.; Garin-Chesa, P.; Lieb, S.; Quant, J.; Grauert, M.; Adolf, G.; Kraut, N.; Peters, J.; Rettig, W. *Curr. Biol.* **2007**, *17*, 316.
3. Benson, C.; Kaye, S.; Workman, P.; Garrett, M.; Walton, M.; de Bono, J. *Br. J. Cancer* **2005**, *92*, 7.
4. Harrington, E. A.; Bebbington, D.; Moore, J.; Rasmussen, R.; Ajose-Adeogun, A.; Nakayama, T.; Graham, J.; Demur, C.; Hercend, T.; Diu-Hercend, A.; Su, M.; Golec, J. M. C.; Miller, K. M. *Nat. Med.* **2004**, *10*, 262.
5. Wilkinson, R. W.; Odedra, R.; Heaton, S. P.; Wedge, S. R.; Keen, N. J.; Crafter, C.; Foster, J.; Brady, M. C.; Bigley, A.; Brown, E.; Byth, K.; Barrass, N. C.; Mundt, K. E.; Foote, K.; Heron, N.; Jung, F. H.; Mortlock, A. A.; Boyle, F. T.; Green, S. *Clin. Cancer Res.* **2007**, *13*, 3682.
6. Zhang, M.; Huck, J.; Hyer, M.; Ecsedy, J.; Manfredi, M. *J. Clin. Oncol.* **2009**, *27*, 8553.
7. DePinto, W.; Chu, X.-J.; Yin, X.; Smith, M.; Packman, K.; Goelzer, P.; Lovey, A.; Chen, Y.; Qian, H.; Hamid, R.; Xiang, Q.; Tovar, C.; Blain, R.; Nevins, T.; Higgins, B.; Luistro, L.; Kolinsky, K.; Felix, B.; Hussain, S.; Heimbrook, D. *Mol. Cancer Ther.* **2006**, *5*, 2644.
8. Kasibhatla, S. R.; Hong, K.; Zhang, L.; Boehm, M. F.; Fan, J.; Le Brazidec, J. Patent WO2008094602, 2008; Patent WO2008094575, 2008.
9. Adams, J.; Kasparec, J.; Silva, D.; Yuan, C. WO03/029209A2, 2003.
10. FRET based AKA and CDK1 Z-lyte Kinase Assays: AKA and CDK1 kinase assays were performed using the Z-lyte platform according to manufacturer's instructions (Invitrogen). Briefly, in the primary kinase reaction, synthetic Z-lyte Peptide Substrate (final concentration 2 μM) is labeled with a donor fluorophore (coumarin) and an acceptor fluorophore (fluorescein). The specific kinase (final concentration 3 nM) then transfers the γ-phosphate of ATP to a single tyrosine, serine, or threonine residue on the substrate. Phosphorylation is suppressed in the presence of a kinase inhibitor (30–0.017 μM). In the secondary development reaction, a site-specific protease (Development Reagent) is added and the development buffer quenches the kinase reaction. Cleavage disrupts FRET between donor and acceptor fluorophores on the non-phosphorylated substrate, while uncleaved, phosphorylated substrate maintains FRET. The fluorescence is measured at 445–520 nm and the % phosphorylated is determined from the ratio of coumarin emission to fluorescein emission. EC_{50s} were determined by GraphPad analysis.
11. G2/M arrest assay: 2×10^4 K562 cells were treated with varying concentrations of compound for 24 h. The cells were then stained by propidium iodide staining buffer (1% sodium citrate, 0.1% Triton X-100, 50 μg/ml propidium iodide in PBS) and analyzed by flow cytometry (5000 events were collected). The Waston model was applied to obtain cell cycle data (FlowJo) and the concentration at which the ratio of G2 peak to M peak was greater than 1 was determined to be the minimum concentration at which G2/M arrest was achieved.
12. Cell proliferation assay: Approximately 2×10^3 Hct116 or K562 cells were seeded in a 96 well plate. After the cells were allowed to adhere overnight, cells were treated with a final concentration of 10–0.01 μM of compound for 5 days. Cell viability was assessed using the tetrazolium-based MTS reagent (Promega) with absorbance measured at 490 nm. EC_{50s} were determined by GraphPad analysis.
13. The coordinates for the X-ray co-crystal structures of compounds **2** and **10e** with AKA at 2.8 Å resolution have been deposited in the PDB. The PDB ID codes are 3R22 and 3R21, respectively.
14. The PyMOL Molecular Graphics System, Version 1.3, Schrödinger, LLC.
15. Bidirectional Transport Assay using Caco-2: Caco-2 cells were purchased from ATCC. Caco-2 cells were grown with media containing high glucose DMEM supplemented with 10% FBS and 1% Non-essential amino acids. Caco-2 cells from passage 25–50 were seeded on a 24-well transwell plate (BD Biosciences, San Diego, CA). Cells were washed and pre-incubated for 30 min at 37 °C with transport buffer containing Hank's Balanced Salt Solution (HBSS), 25 mM HEPES, and 1% DMSO. Compounds were then added either to the apical chamber to measure transport to the basolateral chamber (A–B transport) or to the basolateral chamber to measure transport to the apical chamber (B–A transport) and incubated for 2 h at 37 °C with gentle shaking.
16. Test compounds were incubated in Duplicate Matrix MultiScreen mintubes (Matrix Technologies, Hudson, NH) with liver microsomes (Xenotech, Lenexa, KS). Each assay is performed in 50 mM potassium phosphate buffer, pH 7.4, and 2.5 mM NADPH. Compounds were tested at a final assay concentration of 1.0 μM. The protein concentration in the reaction mix was 1 mg/mL. Compounds were preincubated for 5 min at 37 °C and the metabolic reactions were initiated by the addition of NADPH. Aliquots of 80 μL were removed from the incubation mix at 0, 5 and 30 min after the start of the reaction for screening data. Each aliquot was added to 160 μL acetonitrile for extraction by protein precipitation. These samples were mixed for 1 min by vortexing, and a volume of the mixture was filtered through wells in 0.25 mm glass fiber filter plates by centrifugation at 3000 rpm for 5 min. Sample extracts were analyzed by LC–MS–MS to determine parent compound levels. Percent loss of parent compound was calculated from the peak area at each time point to determine the half-life for test compounds ($T_{1/2}$, min) and clearance ($T_{1/2}$ expressed as percent hepatic blood flow, $\%Q_h$).
17. Cytochrome P450 inhibition was determined with the use of fluorescent probes (2C9: 7-methoxy-4-trifluoromethylcoumarin; 2D6: 3-[2-(*N*, *N*-diethyl-*N*-methylamino)ethyl]-7-methoxy-4-methylcoumarin; 3A4: 7-benzyloxyquinoline and 7-benzyloxy-4-(trifluoromethyl)-coumarin).
18. hERG assessment used the automated PatchXpress 7000A patch clamp robot (Molecular Devices).